JURNAL PENATAAN RUANG
Volume 21 Nomor 1, Mei, 2026
P-ISSN 1907-4972 | E-ISSN 2716-179X
DOI: https://doi.org/10.12962/j2716179X.v21i1.9743

Multitemporal Analysis of Environmental Criticality and Adaptation Strategies in Built-Up Urban Areas of Jember

Dian Aulia Salsabila✉ [1], Ratih Novi Listyawati[1]
[1]Urban and Regional Planning Study Program, University of Jember, Jember, Indonesia

Received: 05/05/2026 | Reviewed: 11/05/2026 | Accepted: 31/05/2026

✉ dianauliasalsa@gmail.com

Abstract: Global warming is an urban problem that affects critical environmental conditions due to the process of urbanization, one of which is the city of Jember. Increased urbanization in the city of Jember is marked by an increase in population density of 100 people/km² in the last five years, which is exacerbated by changes in the natural landscape. The purpose of this study is to analyze the dynamics of environmental criticality in Jember City and its relationship with built-up land in order to formulate appropriate adaptation strategies. This study uses Landsat data to extract Land Surface Temperature (LST), Normalized Difference Vegetation Index (NDVI), and Normalized Difference Built-up Index (NDBI) to produce an Environmental Criticality Index (ECI). In addition, the relationship between built-up land (supervised classification) and ECI is determined through Ordinary Least Squares (OLS) and Geographically Weighted Regression (GWR), and strategies are formulated through the Analytic Hierarchy Process (AHP). The results of the study show that the level of environmental criticality in Jember City has increased by 2,499.36 Ha over ten years (2015-2025). This condition is related to an increase in the area of developed land, as indicated by a higher R-squared value in 2025 of 0,811. The results provided the basis for the AHP assessment, which highlighted climate-responsive spatial planning and enhanced water resource infrastructure management as the priority strategies for addressing environmental criticality.

Keywords: Built-Up Land; Environmental Adaptation Strategies; Environmental Criticality Index; Geographically Weighted Regression; Ordinary Least Squares.

1. Introduction

Global warming is a phenomenon related to the increase in greenhouse gas levels, particularly the increase in carbon dioxide (CO2) concentrations, which affects changes in the Earth's temperature (Kurniawan et al., 2024). The Intergovernmental Panel on Climate Change (IPCC) states that the global average surface temperature change in the 2021-2040 period will reach 1.5°C even under a very low greenhouse gas emission scenario (SSP1-1.9) and is likely or very likely to exceed 1.5°C under higher emission scenarios (IPCC, 2023). In general, the average temperature increase in Indonesia is estimated to be 0.5-3.92°C in 2001 compared to conditions in 1981-2010. Global warming is the result of climate change, which has now become a widespread environmental issue and is not just a problem for individual countries (A Suryansyah et al., 2021).

Climate change due to global warming has negative impacts, such as sea level rise, extreme weather, disruption to crop productivity, and human health (Shivanna, 2022). The impacts of global warming are increasingly felt in Indonesian cities, which are geographically very vulnerable to the effects of climate change (A Suryansyah et al., 2021). This is because urbanization creates a drastic temperature difference between urban areas and surrounding rural areas (Li et al., 2018). Indonesia has shown the dynamics of the urbanization process from 2000 to 2015 through the development of cities, especially on the island of Java (Mardiansjah & Rahayu, 2019). The dynamics of urbanization are also supported by demographic predictions that by 2050, around 75% of Indonesia's population will live in urban areas (WRI Indonesia, 2019). This increase in population has led to a more prominent increase in the supply and demand for developed land (Dinda et al., 2022). Thus, research is needed to assess the environmental criticality of land use change in urban areas so that it does not contribute to global warming and is able to meet land needs.

Approaches to assessing environmental criticality have been extensively studied through the Environmental Criticality Index (ECI). The ECI is an index designed based on the inverse relationship between two parameters, namely Land Surface Temperature (LST) and Normalized Difference Vegetation Index (NDVI) (Senanayake et al. (2013) in Bhattacharyya et al., 2025). Furthermore, the ECI has been developed to be combined with the Normalized Difference Built-up Index (NDBI) (Mallik et al., 2023). The relationship between these three parameters can be correlated with a high ECI value, indicating significant environmental pressure due to excessive development (high NDBI) and minimal vegetation (low NDVI), which causes an increase in surface temperature (high LST) (Malik et al., 2019). This ECI calculation differs from the Urban Heat Island calculation, which involves subtracting NDBI from NDVI. However, However, according to Bhattacharyya et al. (2025), Malik et al. (2019), Aprilia et al. (2021), Jayasinghe et al. (2024), dan Saputra et al. (2023) the literature review has not shown a specific correlation with built-up land. This is because the parameters only focus on ECI analysis or a general comparison of the three parameters. In addition, ECI research results have not shown further studies on efforts to overcome this problem. This gap is the reason why comprehensive spatial environmental vulnerability research is needed.

The urban areas of Jember Regency, which include Kaliwates District, Patrang District, and Sumbersari District, are among the regions in Indonesia experiencing increased urbanization. Urbanization can be defined as the expansion of urban influence in economic, social, psychological, and morphological terms (Rijal & Tahir, 2022). This is in line with urbanization in Jember, which is characterized by higher employment opportunities compared to rural areas, triggering competition between economic strata and increasing population density by 100 people/km2 over the last five years (Hayati & Yuswadi, 2019; Badan Pusat Statistik, 2021-2025). Therefore, Jember City has experienced a change in its natural landscape to built-up land on the outskirts of the city. Based on Rahmah (2019), agricultural land in Jember Regency from 2017 to 2019 has decreased from 209,579.457 ha to 86,618.0081 ha. This event caused an increase in surface temperature of 3.9–4.6°C in Jember Cit (Listyawati & Prasetiyo, 2021). The increase in surface temperature in Jember has impacted the sensitivity of water resources and changes in rainfall (Rustiawan & Muhammad Zaky Ibnu Malik, 2025). Thus, Jember City is experiencing critical environmental conditions.

Based on these conditions, it can be concluded that the city of Jember is experiencing significant environmental pressure due to urbanization, resulting in land conversion to built-up areas, which has led to an increase in surface temperature. This phenomenon requires a more in-depth and contextual approach to understand the dynamics of environmental criticality. Therefore, this study aims to analyze the dynamics of environmental criticality in Jember City and its relationship with the conversion of built-up land to formulate appropriate adaptation strategies. Thus, this study is expected to fill the gaps in previous studies and encourage sustainable development.

2. Methods

The research location is in the Jember Urban Area, which consists of Patrang District, Kaliwates District, and Sumbersari District (see Figure 1) (Perda Kabupaten Jember No. 1 Tahun 2015 tentang RTRW Kabupaten Jember Tahun 2015-2035, 2015). This study used Landsat 8 (OLI/TIRS) sensors in the years 2015 and 2025, which were downloaded directly from the United States Geological Survey (USGS) website and processed using ArcGIS. Landsat 8 (OLI/TIRS) imagery used in this study was acquired during the dry season with Path/Row 117/066, a spatial resolution of 30 m, and projected in UTM Zone 50S based on the WGS 84 datum. Image preprocessing included layer stacking and clipping to the study area boundary. The general methodology used in this study is illustrated in Figure 2 and explained in the following subsections.

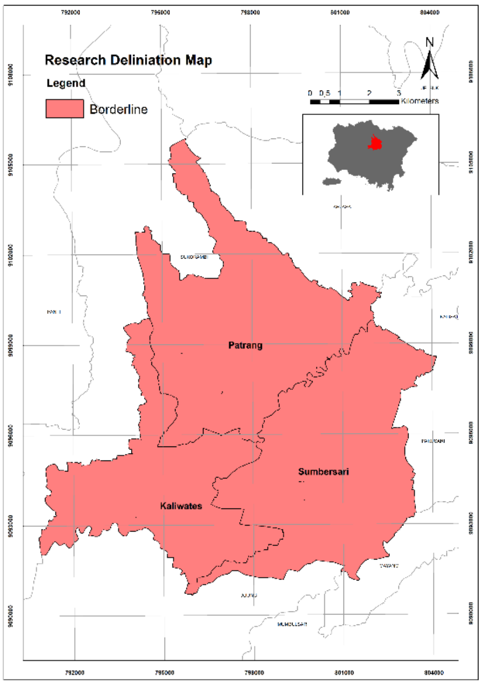

Figure 1. Research Delineation Map

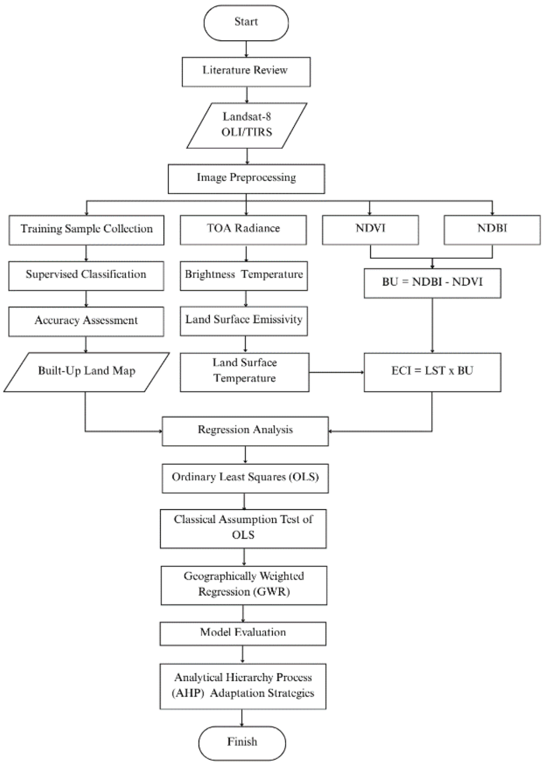

Figure 2. Methodological Flowchart

2.1. Extraction of Built-Up Land

Built-up land is identified through satellite imagery using supervised classification algorithms. The land cover map results are converted into binary classes with a value of 0 for other classes and a value of 1 for built-up land classes. Changes over time in the growth of built-up areas are analyzed separately. Classification accuracy was evaluated using Overall Accuracy (OA) and the Kappa coefficient was calculated using a reference sample obtained from Google Earth imagery (Sim & Yim, 2024).

2.2. Normalized Difference Built-Up Index (NDBI)

NDBI is used as a proxy indicator for urban settlements. In urban areas, reflectance values are typically high in the Short-Wave Infrared (SWIR) band and very low in the Near Infrared (NIR) band (Mallik et al., 2023). Therefore, the SWIR and NIR bands are used to calculate NDBI using the following formula:

$$\text{NDBI} = \frac{(SWIR - NIR)}{(SWIR + NIR)}$$

In NDBI calculations, NDBI values vary between -1 and +1, where higher NDBI values indicate built-up areas and lower values indicate vegetation and water. However, built-up areas from NDBI are identified using thresholds obtained after several iterations (Mallik et al., 2023).

2.3. Normalized Difference Vegetation Index (NDVI)

NDVI is an index that describes the difference between visible light and near-infrared light from vegetation reflectance, so it can be used to estimate green density in a land area (Schinasi et al., 2018).

$$\text{NDVI} = \frac{(NIR - Red)}{(NIR + Red)}$$

NDVI values range from -1 to 1, where a value of 0 or close to 0 indicates land without vegetation, a negative value of -1 or close to -1 indicates water, snow, and others, while positive values close to +1 indicate vegetated land, and positive values close to +1 indicate (Kumari et al., 2022).

2.4. Land Surface Temperature (LST)

LST is the temperature of the surface or surface skin of the earth (Bhattacharyya et al., 2025). Land Surface Temperature (LST) was derived from Landsat 8 Band 10. The digital number (DN) values were first converted into spectral radiance using radiometric rescaling coefficients obtained from the metadata file (MTL). Spectral radiance was subsequently transformed into brightness temperature (BT) using thermal conversion constants (K1 and K2). Land surface emissivity was estimated using the NDVI Threshold Method based on the proportion of vegetation derived from NDVI values. LST was calculated by correcting brightness temperature with the estimated emissivity. The steps in data processing are shown in the flowchart in Figure 3.

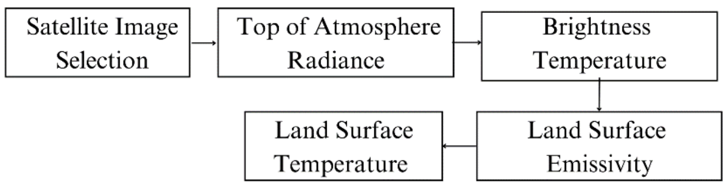

Figure 3. LST Flowchart

Furthermore, LST classification is divided based on thresholds and three quantiles, consisting of low, moderate, and high classifications. The formula for Land Surface Temperature (LST) is as follows:

$$\text{LST} = \text{BT}/(1+(\lambda * \frac{BT}{C2}) * \text{In(E)}$$

λ = radian wavelength : 10,8

E = Surface Emissivity

c2 = 14388 mK

2.5. Environmental Criticality Index (ECI)

ECI is a prerequisite that helps identify areas that deviate from the surrounding environmental conditions. This study calculates ECI by multiplying the BuiltUp (BU) index by LST. The BU index is calculated by subtracting NDVI from NDBI (Mallik et al., 2023). ECI classification is classified based on thresholds and three quantiles, consisting of low, moderate, and high classifications. The formulas are as follows:

$$\text{BU} = \text{NDBI} - \text{NDVI}$$

$$\text{ECI} = \text{LST} \times \text{BU}$$

2.6. Supervised Classification

Supervised classification is a spatial analysis method that uses training sites for each land cover class. With training sites, the algorithm can assign each image pixel to the appropriate class based on its predictor variable values. In the context of remote sensing and land cover, supervised classification can also be defined as a model built based on previously labeled data. The model requires field data as a reference in the process of accurately determining land cover (Natun & Sumarlin, 2025). Pre-labeled data can also be referred to as training samples. Training samples are described in detail as a collection of examples representing each class. From these examples, the algorithm is able to recognize patterns and predict class labels on new data that it has never seen before. This plays an important role in the learning process and the model's ability to generalize, and the quality of the training data greatly affects the accuracy of the classification results (Maxwell et al. (2018) in Moraes et al., 2024).

2.7. Regression Analysis

The regression analysis was conducted using spatial units represented by sub-districts (kecamatan) within the Jember Urban Area. For each spatial unit, the percentage of built-up land was calculated as the independent variable, while the Environmental Criticality Index (ECI) score was used as the dependent variable. The resulting dataset was represented as polygon features with associated attribute values and subsequently used as input for OLS and GWR analyses. Ordinary Least Squares (OLS) regression was initially performed to examine the global relationship between built-up land and ECI. The model was evaluated using R^2, Adjusted R^2, F-statistic, Koenker (BP) statistic, and Jarque-Bera statistic to assess explanatory power, spatial non-stationarity, heteroscedasticity, and residual normality. The results of OLS were subsequently used as the basis for implementing GWR to capture local spatial variations. Geographically Weighted Regression (GWR) was employed to identify local variations in the relationship between built-up land and Environmental Criticality Index (ECI). The model was implemented in ArcGIS using an adaptive kernel approach, where observations closer to a target location received greater weights than those farther away. The optimal bandwidth was automatically determined using the Akaike Information Criterion corrected (AICc) method (Koh et al., 2020). Model performance was evaluated using the coefficient of determination (R^2), adjusted R^2, AICc, residual sum of squares, effective number of parameters, and sigma values.

2.8. Analytical Hierarchy Process (AHP)

AHP is a structured technique for organizing and solving complex decision-making problems through a comprehensive and logical framework to quantify each element of structural decision-making in a hierarchical structure. AHP begins by selecting decision criteria, which are then evaluated based on the selected criteria (Tavana et al., 2023). The consistency of the pairwise comparison matrix was evaluated using the Consistency Ratio (CR), where a CR value below 0.10 indicates acceptable consistency of judgments. This study uses AHP to determine environmental adaptation strategies due to the influence of built-up land on ECI based on Permen PU No. 11/PRT/M/2012 Tentang Rencana Aksi Nasional Mitigasi dan Adaptasi Perubahan Iklim Tahun, 2012. AHP was conducted using purposive sampling techniques on five relevant agency employees, namely Dinas Perumahan Rakyat, Kawasan Permukiman dan Cipta Karya Kabupaten Jember, Dinas Lingkungan Hidup Kabupaten Jember, Kantor Pertanahan Kabupaten Jember (ATR/BPN), Badan Perencanaan Pembangunan Daerah Kabupaten Jember, Badan Penanggulangan Bencana Daerah Kabupaten Jember.

3. Results and Discussion

3.1. Distribution of The Environmental Criticality Index (ECI) in Jember Urban Area

The spatial distribution of Jember Urban NDVI is illustrated in Figures 4. with statistical summaries provided in Table 1. The highest NDVI value shows a decrease from 2015 to 2025 of 0.01. In 2015, the highest value recorded was 0.60, then decreased in 2025 by 0.59. This pattern reflects changes in vegetation cover as indicated by the color density, with lighter colors in 2025. Meanwhile, the minimum value of NDVI shows an increase from -0.03 to -0.005. This indicates an increase in the built-up capacity of the water area in 2025 because the NDVI index value is close to 0. This situation may be influenced by the Kali Jompo area in the city center, which indicates an increase in dry sediment or seasonal drying so that the area can be detected as built-up land. On average, the NDVI value decreased from 2015 to 2025 by 0.01. Furthermore, the standard deviation of NDVI increased by 0.02 over ten years. This indicates that the vegetation condition in Jember City slightly decreased over ten years. A lower NDVI indicates less vegetation or more developed land cover, so the average trend indicates a gradual degradation of vegetation. This condition is illustrated by the distribution of light green colors that tend to spread from the center to the outskirts of the city in Figure 4. Meanwhile, the standard deviation value reflects several locations that are indicated to have experienced a more drastic decline in NDVI, while other locations are relatively stable or have increased slightly, as seen from the difference in changes in the city center and the suburbs.

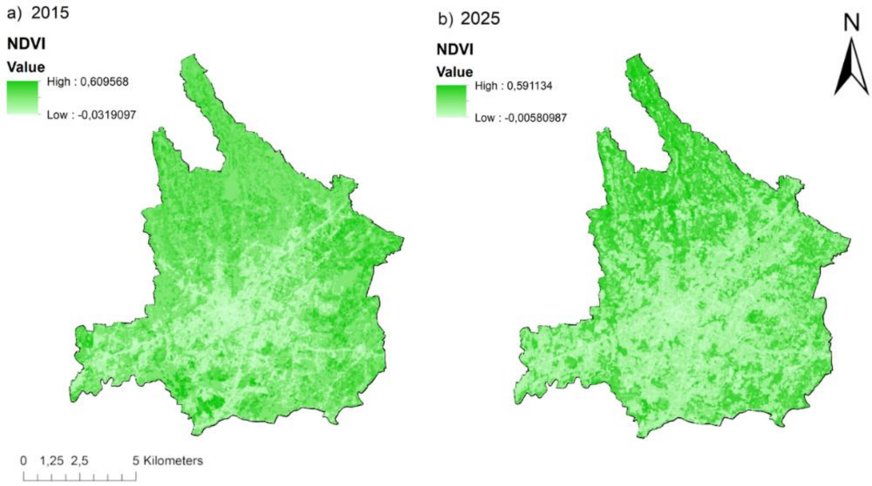

Figure 4. NDVI distribution over 2015, 2025

Table 1. Summary Statistics of NDVI Values in Jember Urban Area

Year	Max	Min	Mean	Standard Deviation
2015	0,60	-0,03	0,29	0,11
2025	0,59	-0,005	0,28	0,12

The NDBI distribution pattern broadly shows consistency with the inverse NDVI distribution pattern shown in the comparison between Figure 4 and Figure 5, where the highest NDBI intensity is found in the urban center, while the highest NDVI intensity is found in the urban periphery, indicated by dark green and dark brown colors. Spatial changes in NDBI are shown in Figure 5 with statistical summaries in Table 2. The calculation results show the dynamics of NDBI distribution in the Jember Urban Area in 2015 and 2025. The maximum NDBI value increased by 0.01 from 2015 to 2025. Meanwhile, the minimum NDBI value remained the same from 2015 to 2025. This can be seen in the color intensity, which changed from lighter to darker. The average NDBI value indicates the dominance of built-up land, which is in line with the average NDVI trend. The average NDBI trend shows an increase of 0.07 (Table 2), which can be seen in Figure 5, where the dark brown area spreads and becomes denser in 2025. This indicates significant urban expansion over the past ten years, both horizontally and vertically in land use patterns. Meanwhile, the increase in the NDBI standard deviation value indicates greater variation in values between pixels, which indicates an increase in the spatial heterogeneity of built-up land conditions (Table 2). This reflects that the urbanization process does not occur evenly but is concentrated in certain locations with varying intensities of development.

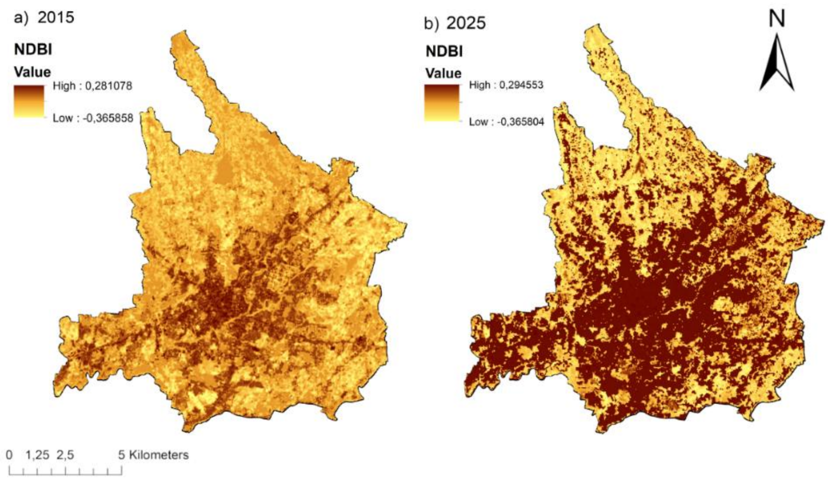

Figure 5. NDBI distribution over 2015, 2025

Table 2. Summary Statistics of NDBI Values in Jember Urban Area

Year	Max	Min	Mean	Standard Deviation
2015	0,28	-0,36	-0,12	0,08
2025	0,29	-0,36	-0,05	0,16

The classification of LST values in 2015 and 2025 shows an increase in the temperature threshold of 0.36°C in Figure 6. This phenomenon indicates that the effect of reduced vegetation cover on increased surface temperature is interrelated in the observed period. This relationship is illustrated by an inverse correlation. An increase in the threshold value indicates that Jember City has experienced a rise in surface temperature, reflecting a decrease in the land's ability to reduce heat. This condition is generally associated with a decrease in vegetation density, so that more solar radiation is absorbed and stored by the land surface. Therefore, the increase in LST threshold can be interpreted as an indicator of vegetation cover degradation that triggers hotter thermal conditions.

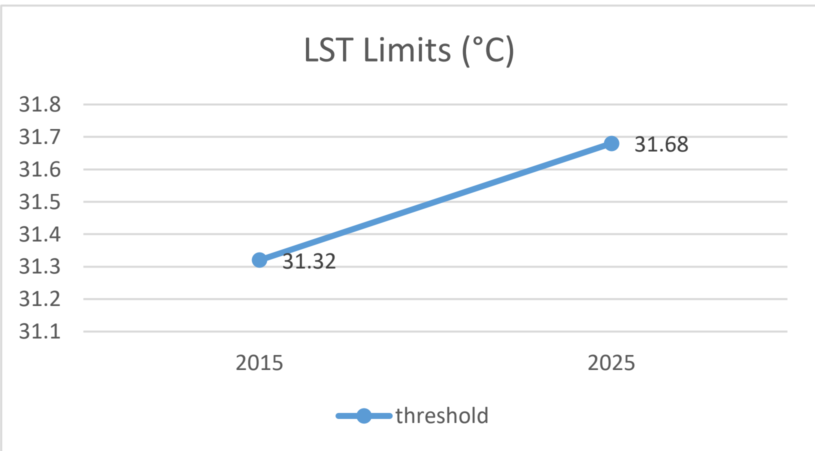

Figure 6. LST Limits

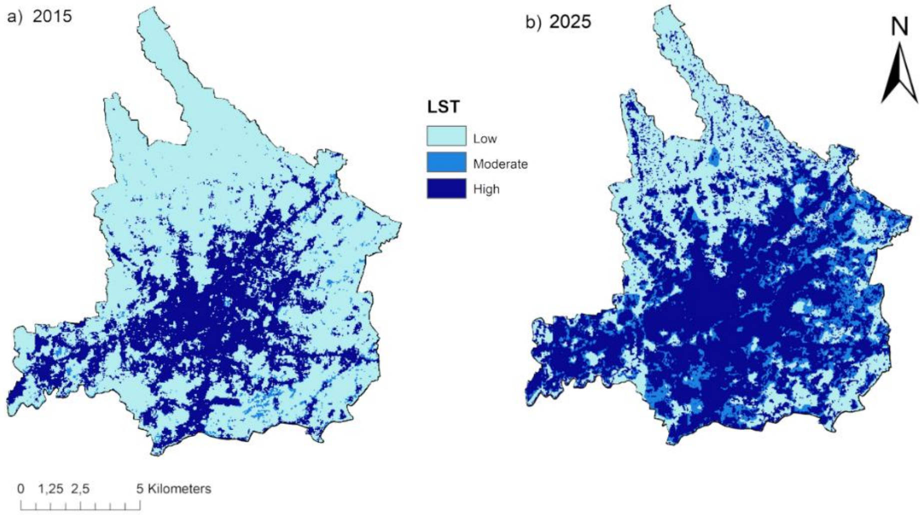

Figure 7. LST distribution over 2015, 2025

The LST classification calculation is divided into three categories based on standard deviation, as shown in Table 3. The LST category indicates a change in the surface temperature range for each class, which is influenced by the threshold. The change in the LST category range shows an upward trend. These values are followed by changes in the distribution of area in each temperature class, as shown in Table 4. The low category shows a decrease of 3,299.72 ha from 2015 to 2025. Meanwhile, the trend for the medium category shows an increase of 1,188.54 ha in 2025. Meanwhile, the trend for the high category shows an increase of 2,131.18 ha over ten years. This phenomenon indicates that urban heat accumulation is significant, with a dominance in the high category over ten years. In 2025, it was identified in detail that the LST condition had a percentage of 51.7% in the high category, 14.09% in the medium category, and 34.21% in the low category.

Table 3. LST (°C) Value Classification in Jember Urban Areas

Description	2015	2025
Low	<28,42	<29,715
Moderate	28,42-31,32	29,715-31,68
High	>31,32	>31,68

Table 4. LST Area (Ha) in Jember City

Description	2015	2025
Low	6.680,30	3.380,58
Moderate	203,31	1.391,85
High	2.977,04	5.108,22

The results of calculating the three parameters of NDV and NDBI (development index) with LST are used to determine the level of environmental criticality of cities as ECI. The distribution of ECI has dynamic values in

2015 and 2025, as shown in Figures 8 and 9. The ECI value limit has increased by 3.755 (Figure 8). This value is reflected in the distribution pattern of the highest intensity, which was yellow in 2015 and changed to a darker red in the urban center and a lighter yellow in 2025 (Figure 9). This shows that the distribution pattern of the highest ECI values is directly related to NBI and LST and inversely related to NDVI. Statistically, conditions in Jember City are becoming increasingly critical, with suburban areas experiencing increasing environmental pressure, which drives the distribution of high ECI values. This is reinforced by the decline in NDVI values, while NDBI and LST values have increased. The combination of a decrease in surface temperature, the spread of development from the city center, and a decline in vegetation has caused ECI values to increase in 2025.

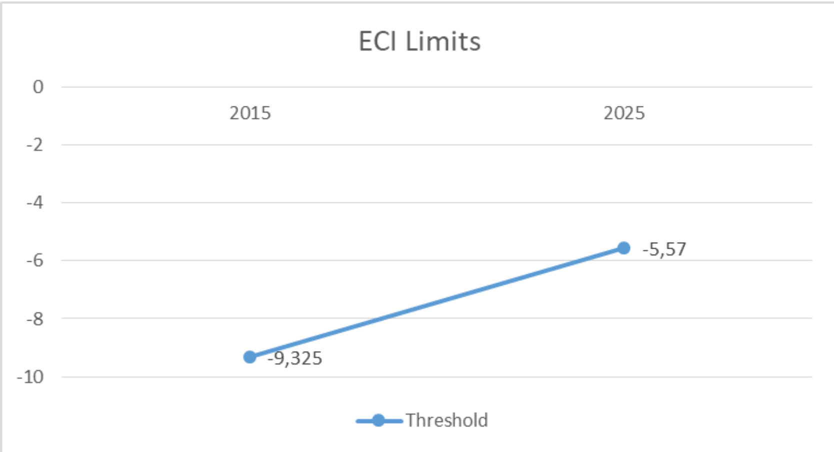

Figure 8. ECI Limits

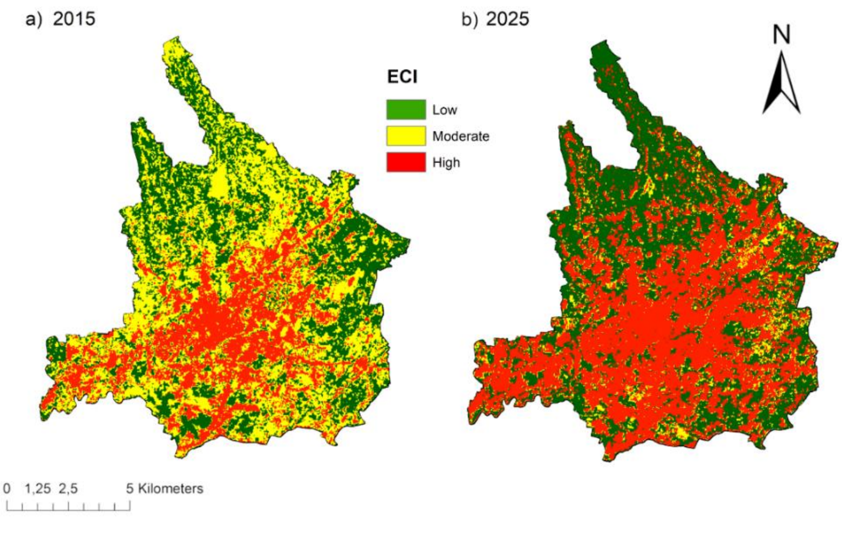

Figure 9. ECI distribution over 2015, 2025

The ECI values in Table 5 show an increase in the area of environmental criticality in 2025. The low category area shows an increase of 972.96 Ha from 2015 to 2025. The medium category area also shows a decrease in 2025 of 3,472.32 Ha. However, the high category area shows a significant increase of 2,499.36 ha over ten years. This is because the moderate environmental criticality conditions in 2015 tended to increase, causing an expansion of the high critical area in Jember City, even though only 972.96 ha experienced recovery. Thus, the dominance of critical areas in 2015 was 25.53%, and in 2025 it will be 50.94%. Over a ten-year period, the area with a high level of criticality has almost doubled compared to the conditions in 2015. This means that environmental pressure in urban areas is significant and the spread of critical areas is becoming more widespread.

Table 5. ECI in Jember Urban Areas (Ha)

Description	2015	2025
Low	3.064,98	4.037,94
Moderate	4.282,14	809,82
High	2.533,53	5.032,89

3.2. The Relationship Between Built-Up Land and Environmental Criticality Index (ECI)

The increase in ECI distribution in the Jember Urban Area was caused by the increasing conversion of built-up land, which led to environmental pressure in the city center. The supervised classification results in Figure 10 show a dynamic distribution pattern from 2015 to 2025. Built-up land areas continue to spread from the city center to the south and north. This distribution pattern is in line with the increasing size of built-up land each year. The area of built-up land in 2015 was 3,273.3 Ha and in 2025 it was 5,007.24 Ha. This indicates an increase in built-up land over 10 years of 52.97%. In addition, the increase in the distribution of built-up land has the same distribution as the NDBI.

The reliability of the built-up land classification results was evaluated using a confusion matrix. The classification for 2015 achieved an Overall Accuracy (OA) of 96% with a Kappa Coefficient of 0.905, while the 2025 classification obtained an OA of 90% and a Kappa Coefficient of 0.800. These results indicate a high level of agreement between the classified maps and the reference data, confirming the reliability of the extracted built-up land information for subsequent spatial analyses. Previous studies using Landsat and Sentinel imagery reported that OA values ranging from 90–94% and Kappa coefficients between 0.81–0.92 represent good to very good classification performance (Aldiansyah & Saputra, 2022). Therefore, the accuracy achieved in this study meets commonly accepted standards for land cover mapping and provides a robust basis for analyzing the relationship between built-up land expansion and environmental criticality in the Jember Urban Area.

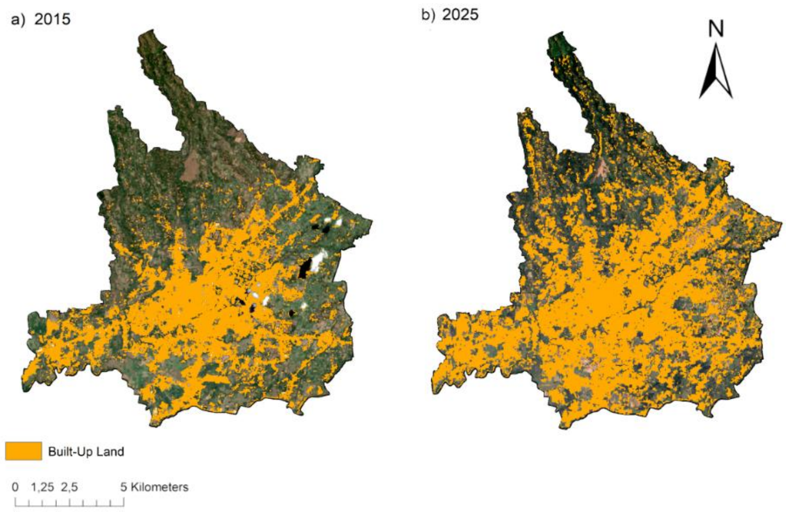

Figure 10. Multitemporal Built-up Land

The relationship between ECI and built-up land was proven by the results of spatial regression analysis using Ordinary Least Squares (OLS) and Geographically Weighted Regression (GWR). In this study, OLS was used as the initial stage of analysis because it was able to provide a general overview. OLS was used to identify the linear relationship between the independent variable (built-up land) and the dependent variable (environmental criticality).

Table 6. OLS Statistical Results

Statistic	2015		2025	
	Value	Probabilitas (p-value)	Value	Probabilitas (p-value)
Multiple R-Square	0,007385	-	0,780150	-
Adjusted R-Squared	0,006887	-	0,780073	-
Joint F-Statistic	14,834821	0,000121	10.113,4055	0,000000
Joint Wald Statistic	17,230660	0,000033	6.756,8982	0,000000
Koenker (BP) Statistic	76,347671	0,000000	530,25915	0,000000
Jarque-Bera Statistic	422,536140	0,000000	2.867,0049	0,000000
Akaike's Information Criterion (AICc)	10.506,178	-	13.958,4212	-

Table 6 shows that the correlation between developed land and environmental criticality has a different magnitude of influence between 2015 and 2025. OLS regression shows a determination (Multiple R-Squared) of 0.007385 and an Adjusted R-Squared of 0.006887 in 2015, while 2025 shows a determination (Multiple R-Squared) of 0.780150 and an Adjusted R Squared of 0.780073. This means that the effect of built-up land on environmental criticality in 2015 shows a weak effect with a percentage of 0.6-0.7%, while in 2025 it shows a strong effect with a percentage of 78%. Meanwhile, the F-statistic and Wald test for both years are highly significant because they have a p-value < 0.01, confirming that built-up land collectively affects environmental criticality. However, there are indications of a violation of the classical OLS assumption because the Koenker (BP) test and Jarque-Bera test have a p-value < 0.01. Koenker (BP) shows heteroscedasticity, meaning that the residual variance is not constant across regions, which can result in biased standard errors and less reliable confidence intervals (Cattaneo et al., 2017). The Jarque-Bera test also indicates that the residuals are not normally distributed, so the assumption of normality may affect the validity of the significance test. Overall, the OLS statistical results are less capable of identifying local variations between regions. For example, regions with high built-up land have different residual patterns than vegetated regions. Thus, the regression process needs to be continued to the GWR model, which can identify coefficients and residual variances that vary according to regional heterogeneity (Mahato et al., 2025).

Table 7. GWR Statistical Results

Statistic	2015	2025
Bandwidth (meter)	2.449,441173	505,215889
Residual Squares	21.338,27214	16.906,01366
Effective Number	19,028069	325,900717
Sigma	3,285333	2,586994
AICc	10.422,5388	13.680,713776
R^2	0,058972	0,832946
R^2 Adjusted	0,050391	0,811459

The GWR modeling results are shown in Table 7, which shows that the local model has better explanatory power than the global OLS model. The R^2 and Adjusted R^2 values for both years are greater than those of the OLS model, with an influence of around 5-5.8% in 2015 and around 81-83% in 2025. The high determination value indicates spatial heterogeneity in the relationship between variables, making the GWR approach more appropriate (Wei et al., Wang et al. in Bawasir et al., 2025). Furthermore, the AICc values are smaller at 10,422.5388 (2015) and 13,680.713776 (2025) compared to the OLS model at 10,506.1780 (2015) and 13,958.4212 (2025). The decrease in the AICc value explains a better balance between explanatory power and model complexity, making the GWR approach more informative (Oshan et al., 2019). In addition, the bandwidth of 2,449.441 and 505.2158 interprets the spatial scale in local weighting, reflecting a more regional pattern (Fotheringham et al., Oshan et al. in Bawasir et al., 2025). The complexity of the model is also shown by the effective numbers of 19.028 and 325.900, which are relatively large and smaller than the number of observations (n=1,996), so the risk of overfitting can be said to be low. Meanwhile, the residual squares values of 21,338.272 and 16,906.01366, as well as sigma values of 3.285 and 2.586, indicate deviations, suggesting that other factors are influencing the results.

Table 8. Comparison of OLS and GWR

Statistic	2015		2025		Interpretation
	OLS	GWR	OLS	GWR	
Multiple R-Square	0,007385	0,058972	0,780150	0,832946	GWR better describes spatial variation.
Adjusted R-Squared	0,006887	0,050391	0,780073	0,811459	GWR remains superior while taking model complexity into account
Akaike's Information Criterion (AICc)	10.506,178	10.422,5388	13.958,421	13.680,713	GWR is more efficient (lower AICc)
Ability to explain spatial variation	Global	*Local* R^2 = 0,00-0,04	Global	*Local* R^2 = 0,07-1,00	GWR is able to capture spatial heterogeneity

A comparative analysis of statistical indicators is presented in Table 8. The OLS model describes the global conditions of the relationship between built-up land and environmental criticality, assuming that the relationship between variables is homogeneous. However, OLS does not ignore significant spatial variations between regions. In contrast, GWR performs better in capturing spatial variations.

Table 9. General Model

		Coefficient	
Year	Sig.	Constant	Built-up land
2015	0,000121	-11,0025	0,587883
2025	0,000000	-13,841575	10,775595

Next, the spatial regression equation shown in Table 9 was obtained. All significance values (Sig.) were less than 0.01, indicating that the relationship between built-up land and ECI was statistically significant. The regression coefficient values for the built-up land variable indicate that an increase in built-up land intensity is associated with a decrease in ECI values, so that areas dominated by built-up land tend to have higher levels of environmental criticality.

The visualization of standardized residuals (Figure 11) illustrates that the OLS model produces fairly large predictions and forms spatial cluster patterns. For example, low built-up land areas have the same value as vegetation areas in 2015. Meanwhile, in 2025, the difference in values between built-up and vegetation areas has extreme residual differences. Therefore, the GWR results are able to capture spatial variations between variables better than OLS. However, the interpretation of local coefficients requires caution due to the potential for detection bias, so GWR results can be supplemented with additional diagnostic analyses (Bawasir et al., 2025).

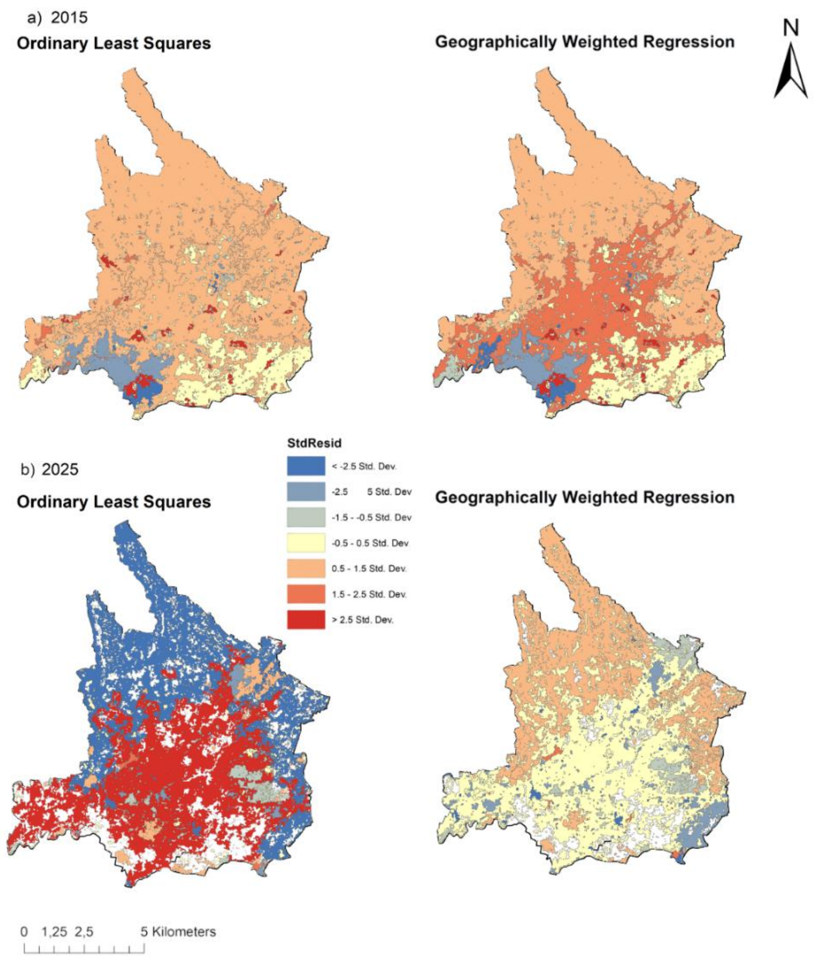

Figure 11. Residual Map

3.3. Priorities for Environmental Criticality Strategies in Jember Urban Area

The priority of environmental criticality strategies was obtained through the Analytical Hierarchy Process (AHP). The environmental criticality strategy used was the environmental adaptation strategy because the distribution of ECI in the Jember Urban Area was related to an increase in the area of built-up land. This analysis was used to compare sub-fields of environmental criticality adaptation strategies consisting of sub-fields of spatial planning and construction, human settlements and infrastructure, and water resources. The comparison results show the priority order of adaptation strategies for handling environmental criticality due to an increase in built-up land, supported by the opinions of experts involved in handling environmental criticality in the Jember Urban Area. Based on the analysis using Expert Choice 11, the priority of environmental criticality adaptation strategies can be seen in Figure 12.

Figure 12. Priority Order of Sub-Areas of Environmental Criticality Adaptation Strategy

Based on Figure 12, the AHP calculation results show that the average total weight value is 0.334. Furthermore, sub-areas are selected based on total weight values above the average. Thus, there are two priority sub-areas in the environmental adaptation strategy in the Jember Urban Area, namely spatial planning and construction with a value of 0.433 and water resources with a value of 0.427. Next, an analysis was conducted on the weighting of the indicators of the three factors using Expert Choice 11.

Figure 13. Priority Strategy for Spatial Planning and Construction

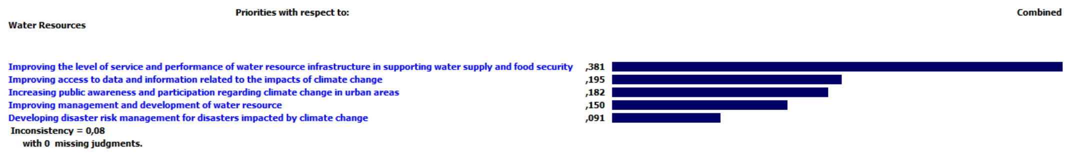

Figure 14. Water Resources Priority Strategy

Figures 13 and 14 show the priority strategies for the selected sub-areas. Figure 13 shows that the priority strategy in the sub-area of spatial planning and construction is improved implementation of integrated programs in the field of public works and spatial planning that are responsive to the impacts of climate change. Meanwhile, Figure 14 shows that the priority strategy in the Water Resources Priority sub-field is improving the level of service and performance of water resource infrastructure in supporting water supply and food security. Thus, two main strategies have been formulated in accordance with the priority sub-fields in adapting to environmental criticality in Jember City due to ECI.

The priority strategies identified through the AHP are consistent with the observed relationship between urban growth and critical environmental levels in the Jember Urban Area. The increase in built-up land between 2015 and 2025 was accompanied by a reduction in vegetation cover and an increase in land surface temperature, which collectively contributed to higher Environmental Criticality Index (ECI) values. This pattern suggests a conceptual pathway in which urban growth intensifies ecological pressure through land cover transformation and thermal stress, thereby increasing environmental criticality and necessitating adaptive policy responses. Previous studies have emphasized that climate-responsive spatial planning should incorporate urban green infrastructure, including residential green spaces, urban vegetation, urban parks, urban forests, street trees, green corridors, green roofs and walls, grasslands, and community gardens to mitigate urban heat and maintain ecological functions (Jia & Turcu, 2025). Furthermore, urban planners are encouraged to optimize the spatial distribution of green infrastructure by prioritizing areas experiencing the highest environmental pressure (Wong et al., 2021). In this context, the priority strategy related to public works and spatial planning reflects the need to integrate green infrastructure and climate adaptation measures into future urban development. At the same time, the priority strategy focused on improving water resource infrastructure highlights the importance of strengthening water availability, ecosystem services, and food security, particularly under increasing environmental stress associated with urbanization and climate change. Therefore, the AHP results demonstrate that effective adaptation to environmental criticality requires an integrated approach combining climate-responsive spatial planning with sustainable water resource management.

4. Conclusion

This study conducted a multitemporal comparative analysis of changes in built-up land cover and surface biophysical characteristics represented by NDVI, NDBI, and LST to understand the dynamics of the

Environmental Criticality Index (ECI) in the Jember Urban Area during the period 2015 to 2025. The mapping results show that LST intensity, NDBI values, and NDVI values directly contribute to increased environmental criticality in the city center. The period from 2015 to 2025 shows an increase in ECI, especially in the city center. Overall, the ECI distribution pattern shows that intensive development in the city center is a major factor in increasing environmental criticality. This can be seen from the 52.97% increase in built-up land over 10 years. The results of regression analysis through OLS and GWR show that built-up land has a significant relationship with increased environmental pressure, with an R^2 value increasing from 2015 to 2025 by 0,811. This shows that the influence of development on ECI is getting stronger along with changes in the spatial structure of the city. These findings conclude that Jember City faces increasing ecological pressure due to land conversion. This condition indicates that uncontrolled urban change can worsen environmental conditions in the future if not intervened through appropriate policies. Therefore, an adaptation strategy is needed to address this issue through AHP. Analysis of strategy priorities points to two main sub-areas that need to be prioritized, namely spatial planning and construction, and water resources. The strategy emphasizes improved implementation of integrated programs in the field of public works and spatial planning that are responsive to the impacts of climate change, and improving the level of service and performance of water resource infrastructure in supporting water supply and food security.

References

A Suryansyah, S., Kastolani, W., & Somantri, L. (2021). Scientific thinking skills in solving global warming problems. *IOP Conference Series: Earth and Environmental Science*, *683*(1). https://doi.org/10.1088/1755-1315/683/1/012025

Aldiansyah, S., & Saputra, R. A. (2022). Comparison of Machine Learning Algorithms for Land Use and Land Cover Analysis Using Google Earth Engine (Case Study: Wanggu Watershed). *International Journal of Remote Sensing and Earth Sciences*, *19*(2), 197–210.

Aprilia, H. C., Jumadi, J., & Mardiah, A. N. . (2021). Environmental Critical Analysis of Urban Heat Island Phenomenon Using ECI (Environmental Critically Index) Algorithm in Surakarta City and Its Surroundings. *International Journal for Disaster and Development Interface*, *1*(1), 1–15. https://doi.org/10.53824/ijddi.v1i1.4

Badan Pusat Statistik. (n.d.). *Kabupaten Jember dalam Angka 2021-2025*.

Bhattacharyya, S., Sinha, S., Kumari, M., & Mishra, V. N. (2025). *Spatio-Temporal Influences of Urban Land Cover Changes on Thermal-Based Environmental Criticality and Its Prediction Using CA-ANN Model over Kolkata (India)*. 1–29.

Cattaneo, M. D., Jansson, M., & Newey, W. K. (2017). Inference in Linear Regression Models with Many Covariates and Heteroscedasticity. *Journal of the American Statistical Association*, *113*(523), 1350–1361.

Dinda, R., Mariati, H., & Fitriawan, D. (2022). Analisis Proyeksi Penduduk Dan Alokasi Kebutuhan Lahan Permukiman Di Kota Padang 2020-2030. *Jurnal Azimut*, *4*(1), 19. https://doi.org/10.31317/jaz.v4i1.790

Hayati, A., & Yuswadi, H. (2019). Pola Hubungan Ketetanggaan di Masyarakat Urban: Studi Kasus di Kampung Osing, Jember (The Pattern of Neighbourhood Relation in Urban Society: Case Study in Kampung Osing, Jember). *E-SOSPOL*, *1*, 14–20.

IPCC. (2023). *CLIMATE CHANGE 2023: Summary Synthesis Report for Policymakers*.

Jayasinghe, C. B., Withanage, N. C., Mishra, P. K., Abdelrahman, K., & Fnais, M. S. (2024). Evaluating Urban Heat Islands Dynamics and Environmental Criticality in a Growing City of a Tropical Country Using Remote-Sensing Indices: The Example of Matara City, Sri Lanka. *Sustainability (Switzerland)*, *16*(23). https://doi.org/10.3390/su162310635

Jia, Y., & Turcu, C. (2025). Climate, Health, and Urban Green Infrastructure: The Evidence Base and Implications for Urban Policy and Spatial Planning. *International Journal of Environmental Research and Public Health*, *22*(12). https://doi.org/10.3390/ijerph22121842

Koh, E.-H., Lee, E., & Lee, K.-K. (2020). Application of geographically weighted regression models to predict spatial characteristics of nitrate contamination: Implications for an effective groundwater management strategy. *Journal of Environmental Management*, *268*, 1–12.

Kumari, M., Somvanshi, S., Sharma, R., & Zubair, S. (2022). Analysis, of multi-temporal remotely sensed spectral indices influence on ecology of Singrauli sub-district, Madhya Pradesh using an ecological impact index. *Egyptian Journal of Remote Sensing and Space Science*, *25*(3), 863–871. https://doi.org/10.1016/j.ejrs.2022.08.005

Kurniawan, J., Razak, A., Syah, N., Diliarosta, S., Azhar, A., Studi, P., Lingkungan, I., Sarjana, S. P., & Padang, U. N. (2024). *Pemanasan Global : Faktor , Dampak dan Upaya Penanggulangan*. *3*(6), 646–655. https://doi.org/10.55123/insologi.v3i6.4627

Li, G., Zhang, X., Mirzaei, P. A., Zhang, J., & Zhao, Z. (2018). Urban heat island effect of a typical valley city in China: Responds to the global warming and rapid urbanization. *Sustainable Cities and Society*, *38*, 736–745. https://doi.org/10.1016/j.scs.2018.01.033

Listyawati, R. N., & Prasetiyo, P. (2021). Analysis of Urban Heat Island Phenomenon as A Global Warming Control Based on Remote Sensing in Jember Urban, Indonesia. *IOP Conference Series: Earth and Environmental Science*, *887*(1). https://doi.org/10.1088/1755-1315/887/1/012002

Mahato, R. K., Htike, K. M., Koro, A. B., Yadav, R. K., Sharma, V., Kafle, A., & Ojha, S. C. (2025). Spatial autocorrelation with environmental factors related to tuberculosis prevalence in Nepal, 2020–2023. *Infectious Diseases of Poverty*, *14*(15), 1–24. https://doi.org/https://doi.org/10.1186/s40249-025-01283-y

Malik, M. S., Shukla, J. P., & Mishra, S. (2019). Relationship of LST, NDBI and NDVI using landsat-8 data in Kandaihimmat watershed, Hoshangabad, India. *Indian Journal of Geo-Marine Sciences*, *48*(1), 25–31.

Mallik, R., Dikkila Bhutia, K., Roy, S., Nandi, M., Dash, P., & Mukherjee, K. (2023). Spatio-temporal Analysis of Environmental Criticality: Planned Versus Unplanned Urbanization. *IOP Conference Series: Earth and Environmental Science*, *1164*(1). https://doi.org/10.1088/1755-1315/1164/1/012014

Mardiansjah, F. H., & Rahayu, P. (2019). Urbanisasi dan Pertumbuhan Kota-Kota di Indonesia: Suatu Perbandingan Antar-Kawasan Makro Indonesia. *Jurnal Pengembangan Kota*, *7*(1), 91–110.

Perda Kabupaten Jember No. 1 Tahun 2015 tentang RTRW Kabupaten Jember Tahun 2015-2035, peraturan.bpk.go.id 1 (2015).

Permen PU No. 11/PRT/M/2012 Tentang Rencana Aksi Nasional Mitigasi dan Adaptasi Perubahan Iklim Tahun, Peraturan Menteri Pekerjaan Umum 1 (2012).

Rahmah, R. A. (2019). *Alih Fungsi Lahan Pertanian Menjadi Perumahan di Kabupaten Jember*. 1–50. https://repository.unej.ac.id/handle/123456789/98849

Rijal, S., & Tahir, T. (2022). Analisis Faktor Pendorong Terjadinya Urbanisasi di Wilayah Perkotaan (Studi Kasus Wilayah Kota Makassar). *Journal of Economic Education and Entrepreneurship Studies*, *3*(1), 262–276.

Rustiawan, I. Z., & Muhammad Zaky Ibnu Malik. (2025). Pengaruh Globalisasi dan Perubahan Iklim Global terhadap Sumber Daya Air dan Lahan di Kabupaten Jember, Jawa Timur. *Jurnal Pengabdian Masyarakat dan Riset Pendidikan*, *4*(1), 869–879. https://doi.org/10.31004/jerkin.v4i1.1667

Saputra, L. I. A., Jumadi, & Sari, D. N. (2023). *Analysis of Environmental Criticality Index (ECI) and Distribution of Slums in Yogyakarta and Surrounding Areas Using Multitemporal Landsat Imagery* (Nomor 2). Atlantis Press SARL. https://doi.org/10.2991/978-2-38476-066-4_26

Schinasi, L. H., Benmarhnia, T., & De Roos, A. J. (2018). Modification of the association between high ambient temperature and health by urban microclimate indicators: A systematic review and meta-analysis. *Environmental Research*, *161*(September 2017), 168–180. https://doi.org/10.1016/j.envres.2017.11.004

Shivanna, K. R. (2022). Climate change and its impact on biodiversity and human welfare. *Proceedings of the Indian National Science Academy*, *88*(2), 160–171. https://doi.org/10.1007/s43538-022-00073-6

Sim, W., & Yim, J. (2024). *Assessing Land Cover Classification Accuracy : Variations in Dataset Combinations and Deep Learning Models*.

Tavana, M., Soltanifar, M., & Santos-Arteaga, F. J. (2023). Analytical hierarchy process: revolution and evolution. *Annals of Operations Research*, *326*(2), 879–907. https://doi.org/10.1007/s10479-021-04432-2

Wong, N. H., Tan, C. L., Kolokotsa, D. D., & Takebayashi, H. (2021). Greenery as a mitigation and adaptation strategy to urban heat. *Nature Reviews Earth & Environment*, *2*(3), 166–181. https://doi.org/10.1038/s43017-020-00129-5

WRI Indonesia. (2019). *Seizing Indonesia's Urban Opportunity Compact, Connected, Clean and Resilient Cities as Drivers of Sustainable Development*.